PHILOSOPHICAL TRANSACTIONS B

royalsocietypublishing.org/journal/rstb

Research

Cite this article: Zeng F, Wunderer J, Salvenmoser W, Ederth T, Rothbächer U. 2019 Identifying adhesive components in a model tunicate. *Phil. Trans. R. Soc. B* **374**: 20190197.
http://dx.doi.org/10.1098/rstb.2019.0197

Accepted: 11 July 2019

One contribution of 15 to a theme issue 'Transdisciplinary approaches to the study of adhesion and adhesives in biological systems'.

Subject Areas:
developmental biology

Keywords:
tunicate, larval adhesion, papillae, lectins, DOPA, heparin

Author for correspondence:
Ute Rothbächer
e-mail: ute.rothbaecher@uibk.ac.at

Electronic supplementary material is available online at https://dx.doi.org/10.6084/m9.figshare.c.4587200.

THE ROYAL SOCIETY PUBLISHING

Identifying adhesive components in a model tunicate

Fan Zeng[1], Julia Wunderer[1], Willi Salvenmoser[1], Thomas Ederth[2] and Ute Rothbächer[1]

[1]Department of Evolutionary Developmental Biology, Institute of Zoology, University Innsbruck, Technikerstrasse 25, 6020 Innsbruck, Austria
[2]Division of Molecular Physics, Department of Physics, Chemistry and Biology (IFM), Linköping University, 581 83 Linköping, Sweden

FZ, 0000-0002-5506-1818; JW, 0000-0003-2425-8009; WS, 0000-0003-3361-0326; TE, 0000-0002-1639-5735; UR, 0000-0002-9989-6139

Tunicates populate a great variety of marine underwater substrates worldwide and represent a significant concern in marine shipping and aquaculture. Adhesives are secreted from the anterior papillae of their swimming larvae, which attach and metamorphose into permanently adhering, filter-feeding adults. We recently described the cellular composition of the sensory adhesive organ of the model tunicate *Ciona intestinalis* in great detail. Notably, the adhesive secretions of collocytes accumulate at the tip of the organ and contain glycoproteins. Here, we further explore the components of adhesive secretions and have screened for additional specificities that may influence adhesion or cohesion of the *Ciona* glue, including other carbohydrate moieties, catechols and substrate properties. We found a distinct set of sugar residues in the glue recognized by specific lectins with little overlap to other known marine adhesives. Surprisingly, we also detect catechol residues that likely originate from an adjacent cellular reservoir, the test cells. Furthermore, we provide information on substrate preferences where hydrophobicity outperforms charge in the attachment. Finally, we can influence the settlement process by the addition of hydrophilic heparin. The further analysis of tunicate adhesive strategies should provide a valuable knowledge source in designing physiological adhesives or green antifoulants.

This article is part of the theme issue 'Transdisciplinary approaches to the study of adhesion and adhesives in biological systems'.

1. Introduction

Marine organisms have developed diverse methods of underwater adhesion as survival strategies, and their adhesives inspire the design of tissue-compatible glues. However, the synthetic homologs insufficiently mimic the underwater properties of the natural glues, and a deeper understanding of the biological complexity of glue composition and deposition will be instrumental in the preparation of the next generation of synthetic homologs [1,2]. The permanent adhesives of adult mussels, barnacles and tubeworms are the best-studied [1,3,4] and the temporary adhesives of echinoderms and flatworms have gained more recent attention [5–7]. Most challenging, however, remain adhesive secretions of marine larvae that are generally small and produce minute quantities of glue, making their efficient analyses very difficult. High-end visualization technologies have recently advanced the analyses of larval glue strategies of barnacle and mussel larvae, revealing very different adhesive strategies from those of the adults [8]. Marine larvae ensure the dispersal, and during initial attachment attempts inspect the substrate for a favourable environment. Settlement triggers a metamorphosis to the often permanently adhering adult, such as for most tunicates. Larval attachment studies thus not only bear the potential for novel adhesive formulations but are crucial

to find green anti-adhesives to prevent biofouling, including that of the widespread and invasive tunicates [9]. Well-developed model organisms such as the solitary tunicate ascidian *Ciona intestinalis* will offer additional entry points to study larval adhesion, taking advantage of an established developmental and functional genomics toolbox [10]. Unlike other marine larvae, ascidian larvae resemble the vertebrate tadpoles in tissue composition and genome sequence, with accumulating molecular developmental knowledge to explain events upstream and downstream of larval attachment, i.e. adhesive organ formation and metamorphosis, respectively. Larval adhesion has been mostly studied from the perspective of metamorphosis, with several molecular milestones separating the steps in the metamorphosis [11,12]. The nature of the initial adhesive secretions, however, remain largely unknown. We have recently reanalysed the *Ciona* larval adhesive organs with an eye on bioadhesion research, and in combination with advanced imaging and functional genomics approaches, documented the detailed three-dimensional organization of the sensory adhesive papillae in terms of cellular composition, molecular markers and ultrastructural details [13]. Among others, we have discovered two types of vesicles in the glue-secreting collocytes, and carbohydrate moieties bound by the lectin peanut agglutinin (PNA) within both the collocytes and the adhesive prints.

Here, we analyse more deeply the ascidian larval adhesive strategies with respect to sugars and adhesive functionalities known from marine organisms. In carbohydrate profiling, we find additional sugar residues present in both the *Ciona* papillae and their adhesive deposits, and conserved within tunicates. Hydrophobic surfaces are clearly preferred in attachment, although the glue deposition is possible on charged hydrophilic substrates, with neutral hydrophilic surfaces being incompatible with larval adhesion. We discovered L-DOPA to be actively uptaken by the papillae, although stored in the neighbouring test cells of the surrounding tunic, but likely released during substrate touching and glue deposition. Strongly hydrophilic heparin and an excess of L-DOPA in the medium blocks adhesion. We discuss possible roles for dihydroxyphenylalanine (DOPA) in adhesion/cohesion and the coordination of subsequent metamorphosis steps.

2. Results

(a) Carbohydrate localization in adhesive organs of swimming larvae

We have previously shown the binding of PNA to the adhesive-secreting collocytes of the tunicate ascidian *C. intestinalis* larvae [13]. To obtain a more complete picture of the carbohydrate moieties possibly involved in the larval attachment of *Ciona*, we screened 21 lectins featuring various sugar specificities (table 1). Lectin binding to fixed larvae was visualized by a lectin-biotin and streptavidin-fluorescence sandwich method followed by fluorescence microscopy (figure 1; electronic supplementary material, figure S1).

Strongest staining in adhesive organs was detected for PNA, *Phaseolus vulgaris* erythroagglutinin (PHA-E) and *Griffonia (Bandeiraea) simplicifolia* II (GSL II) (figure 1*a–c*). PHA-E binding was restricted to the papillary tips (figure 1*b*″) while PNA and GSL II staining extended into the papillary body (figure 1*a*″ and *c*″) and stained additional cell types in the trunk and tail epidermis, respectively (figure 1*a*′ and *c*′). Weaker binding to papillae was detected by *Datura stramonium* (DSL), wheat germ agglutinin (WGA) and concanavalin A (ConA) (figure 1*d–f*). The latter three lectins were less specific and bound significantly to additional structures surrounding the entire larva, like the inner compartment layer (figure 1*d*′) and the two tunic layers (figure 1*d*′–*f*′). The tunic is made of polysaccharides resembling cellulose and it is, therefore, not surprising that the majority (seven) of the remaining lectins bound to the tunic (electronic supplementary material, figure S1), including GSL I, jacalin, LCA, LEL, SBA, STL, VVL and PSA. Alternative specific binding, like the dorsal nerve cord and notochord, was seen for UEAI and nuclear binding for EBL (electronic supplementary material, figure S2). A further five lectins (MAL II, RCA I, SJA, EBL/ECA and PHA-L) did not bind to *Ciona* larvae. Overall, we found three lectins (PNA, PHA-E and GSL II) that specifically mark the *Ciona* larval adhesive organs.

(b) Carbohydrate presence in adhesive prints

The anterior tip of the larval adhesive organ (the hyaline cap) represents a glue reservoir and some of its content is secreted as adhesive patches upon touching and exploring the substrate. Initial adhesion may lead to stable papillary attachment and subsequent metamorphosis. During the initial phase, larvae can be detached easily through a seawater flow from pipetting, and attachment prints are left behind on the surface. We have analysed these adhesive plaques for both the presence of the carbohydrates detected in the adhesive papillae and their shape (figure 2).

Indeed, all three lectins, PNA, PHA-E and GSL II, bound the adhesive plaques (figure 2*a–c*) with very similar distribution, often concentrated in three patches likely secreted from the three papillae, overall forming a rounded area probably caused by a circular movement for glue dispersal within the triangular field of the papillae (see also figure 4*c*).

A similar shape of glue dispersal patches was observed by scanning electron microscopy (SEM) (figure 2*d*,*e*). A thin film of glue was spread out towards the periphery forming a meshwork structure partially ruptured when washing away the larvae for SEM preparations (figure 2*d*). Some patches may present a lengthened central stem of glue material likely extending during larval removal (figure 2*b*, *e*). Scanning imaging of an attached larva showed a similarly shaped material spread on the substrate in the vicinity of the three papillae at the anterior tip of the head (figure 2*f*). The papillae, therefore, secrete a carbohydrate-containing viscous material that spreads out as a thin meshwork to connect the larva to the substrate.

(c) Conserved carbohydrate moieties in distantly related tunicate papillae

To find if such sugar moieties may represent a commonality across tunicates we probed for the presence of the two most specific *Ciona* papillary carbohydrates in the larval papillae of two other tunicates, the solitary ascidian *Phallusia mammillata* and the colonial ascidian *Botryllus schlosseri*. Interestingly, both showed PNA and PHA-E enriched in

Table 1. List of lectins used to stain *Ciona intestinalis* larvae: tissues labelled, intensity and sugar specificity. Notes: (–) no staining, (+) very weak, + weak labelling, ++ intermediate labelling, +++ strong labelling.

lectins	acronym	papillae	tunic	test cells	trunk cells	epidermis cells	notochord nerve cord	nuclei	sugar specificity
peanut agglutinin	PNA	+++	–	–	++	–	–	–	Galβ3GalNAc
Phaseolus vulgaris erythroagglutinin	PHA-E	+++	–	–	–	–	–	–	Galβ4GlcNAcβ2Manα6 (GlcNAcβ4) (GlcNAcβ4Manα3) Manβ4
Griffonia (Bandeiraea) simplicifolia II	GSL II	+++	–	–	+	+	–	–	α or βGlcNAc
Datura stramonium	DSL	++	+	–	–	–	–	–	(GlcNAc)2–4
wheat germ	WGA	+	++	–	–	–	–	–	GlcNAc
concanavalin A	ConA	+	++	++	–	–	–	–	αMan, αGlc
Griffonia (Bandeiraea) simplicifolia I	GSL I	–	++	–	–	–	–	–	αGal, αGalNAc
jacalin	jacalin	–	++	–	–	–	–	–	Galβ3GalNAc
Lens culinaris	LCA	–	++	–	–	–	–	–	αMan, αGlc
soybean	SBA	–	++	–	–	–	–	–	α>βGalNAc
Solanum tuberosum	STL	–	++	–	–	–	–	–	(GlcNAc)2–4
Vicia villosa agglutinin	VVL	–	+++	–	–	–	–	–	GalNAc
Lycopersicon esculentum	LEL	–	+++	(+)	–	–	–	–	(GlcNAc)2–4
Pisum sativum	PSA	–	++	(+)	–	–	–	–	αMan, αGlc
Ulex europaeus I	UEA I	–	–	–	–	–	++	–	αFuc
Sambucus nigra	EBL, SNA	–	–	–	–	–	–	++	Neu5Acα6Gal/GalNAc
Erythrina cristagalli	ECL	–	–	–	–	–	–	–	Galβ4GlcNAc
Ricinus communis I	RCA I	–	–	–	–	–	–	–	Gal
Maackia amurensis II	MAL II	–	–	–	–	–	–	–	Neu5Acα3Galβ4GalNAc
Phaseolus vulgaris leucoagglutinin	PHAL-L	–	–	–	–	–	–	–	Galβ4GlcNAcβ6 (GlcNAcβ2Manα3) Manα3
Sophora japonica	SJA	–	–	–	–	–	–	–	βGalNAc

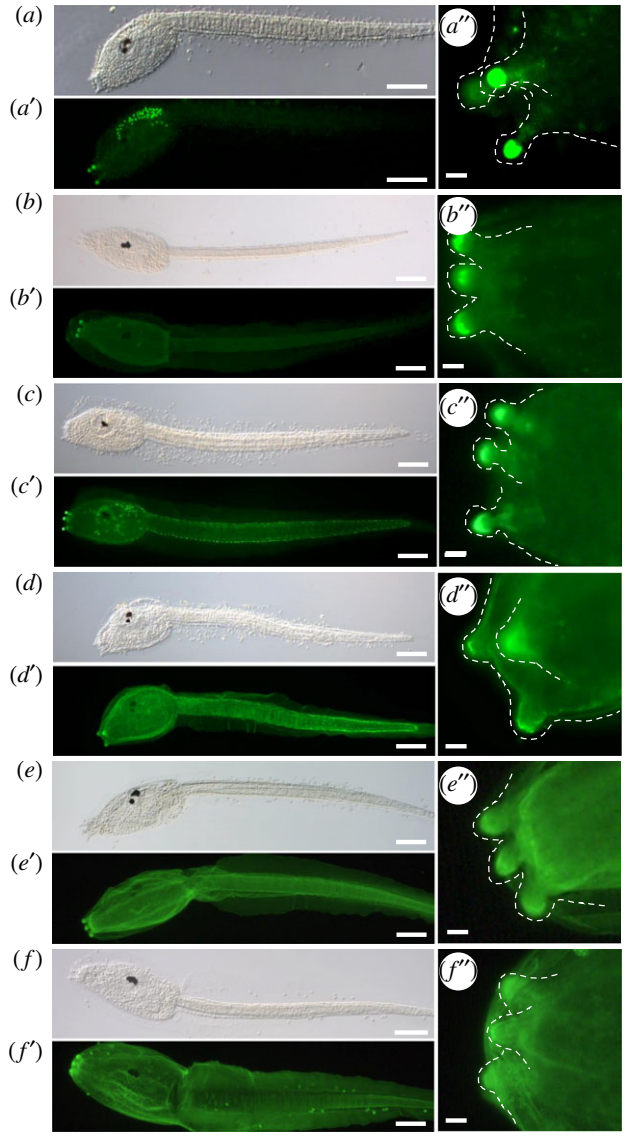

Figure 1. Enrichment of PNA, PHA-E and GSL II bound carbohydrates in the adhesive organs of *Ciona intestinalis* larvae. Fluorescent lectin labelling of *C. intestinalis* larvae with: (*a*-*a*″) PNA, (*b*-*b*″) PHAL-E, (*c*-*c*″) GSL II, (*d*-*d*″) DSL, (*e*-*e*″) WGA and (*f*-*f*″) ConA. Corresponding bright-field images (*a*–*f*), fluorescence (*a*′–*f*′) and details of the papillae (*a*″–*f*″), highlighted by a dashed line, anterior to the left. Scale bars: (*a*–*f*, *a*′–*f*′) 100 μm, (*a*″–*f*″) 10 µm. (Online version in colour.)

their papillae (figure 3) pointing to a more global importance of these specific sugar moieties in the tunicate larval adhesives.

(d) Substrate preferences for larval attachment

While *Ciona* larvae are promiscuous in their choice of substrates in the wild, their preferences become quickly obvious under laboratory conditions where they prefer plastic (polystyrene) over glass or agarose. To define these substrate preferences more precisely, we observed their attachment to different artificial but chemically well-defined substrates or with different additives in the seawater (figure 4). For this purpose, we used self-assembled monolayers (SAMs) of functionalized alkanethiols, which is a well-established method of interfacial engineering [14], with applications also in marine biofouling and bioadhesion studies [15–17].

First, we placed SAMs with hydrophobic (C16), and hydrophilic neutral (EG6), cationic (NH_2) and anionic (MHA) properties on agarose-coated dishes filled with artificial seawater, added around 200 *Ciona* larvae and monitored their preferred attachment to these surfaces, with the initial adhesion being scored within 10 min and stable adhesion after 2 h (figure 4*a*). Initially, most larvae preferred the hydrophobic substrate but to a lesser extent also attached to the anionic surface, while very few and none were found on the cationic or neutral hydrophilic surfaces, respectively (figure 4*b*, grey bars). Two hours later, the larvae had almost unanimously attached stably to the hydrophobic surface and had abandoned the anionic and cationic surfaces (figure 4*b*, dark bars). As usual, many larvae at this stage also attached to each other or to the water surface (not counted).

When we visualized the adhesive plaques on the different SAMs in PNA fluorescence (described in §2a), we detected footprints on the hydrophobic and on both types of charged surfaces (figure 4*c*). The plaques on the hydrophobic surface seemed spread out as a fine circle surrounding the common thicker glue patches in the centre (figure 4c_1 and c_1′). The adhesive plaques on the charged surfaces resembled the central glue patches on the hydrophobic surface (figure 4c_2 and c_3). By contrast, the hydrophilic uncharged surface EG6 contained no PNA-stained adhesive prints (not shown) suggesting that attachment was either not possible or that the glue does not contain carbohydrates.

To further explore the role of hydrophilicity and charge in larval attachment, we tested for any effects of dissolved hydrophilic and polyanionic heparin on adhesion (figure 4*d*). Indeed, 2.5% heparin in the seawater could completely block larval adhesion, with 100% of larvae that remained swimming (figure 4*d*, orange) compared to 80% of larvae having attached in the control (figure 4*d*, blue). To test whether added charge alone could block the larval adhesion we compared increasing concentrations of heparin to increasing amounts of charged amino acids in the seawater (figure 4*e*). Clearly, only minor effects were seen upon the addition of 1, 2, 3 or 4% of the negatively charged aspartic or glutamic acids and positively charged lysine or arginine. At 5% amino acid addition the larvae did not attach but appeared abnormally swollen and unhealthy. Heparin, by contrast, consistently blocked the larval attachment even at the lowest concentrations. Because we noted different wetting of the plastic surface by the heparin solution as compared to the amino acid solutions (electronic supplementary material, figure S3 and movie S1), we suggest that the attachment block is caused by the increased surface hydrophilicity of the plastic dish containing the heparin solution. Taken together, our data point to a clearly favourable role of substrate hydrophobicity in glue deposition and attachment while charge may play a more minor role.

(e) Catechol detection in adhesion competent larvae and their adhesive prints

DOPA residues are well known to play a role in adhesion and glue cohesion of several marine organisms and are found in haemocytes involved in tunic wound healing of adult ascidians [18]. We explored the presence of DOPA in adhesion-competent *Ciona* larvae and their adhesive plaques by, firstly, adapting a protocol used to stain DOPA in haemocytes and, secondly, by an L-DOPA-specific antibody (figure 5).

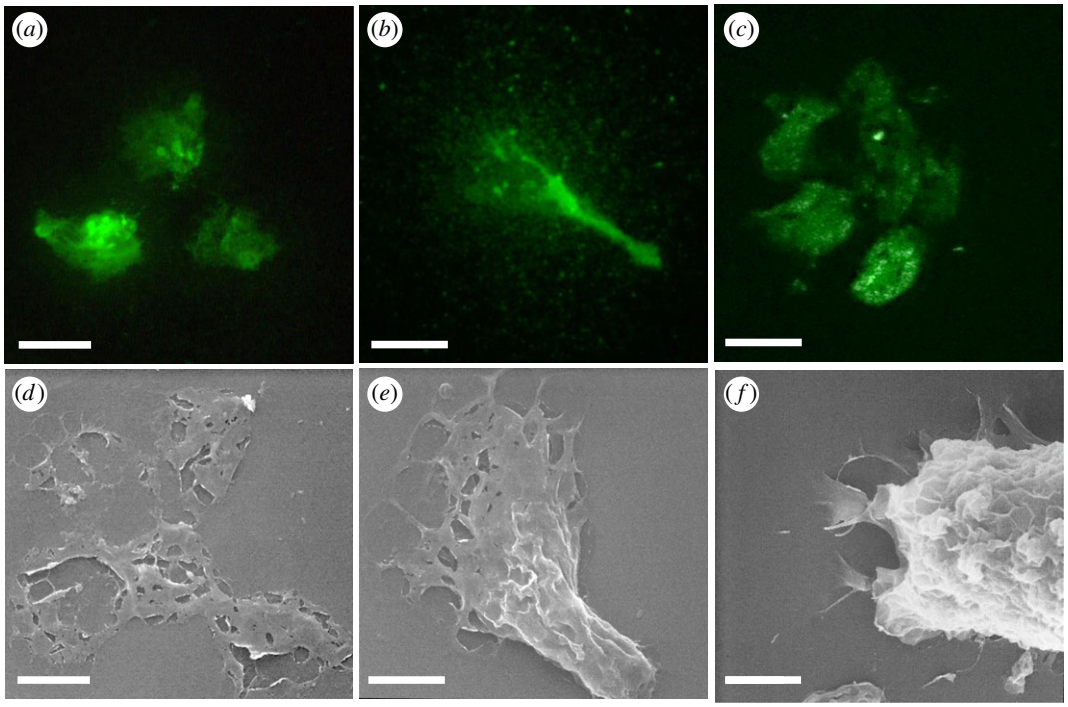

Figure 2. The presence of PHA-E and GSL II bound carbohydrates in the adhesive plaques of *C. intestinalis* larvae. (*a–c*) Confocal images of lectin-fluorescent stainings and (*d–f*) SEM images of adhesive plaques. (*a*,*b*) GSL II and (*c*) PHAL-E staining. (*d*,*e*) SEM pictures of similarly shaped adhesive plaques. (*f*) Substrate attached larva secreting glue from the adhesive papillae. SEM, scanning electron microscopy. Scale bar: 10 µm.

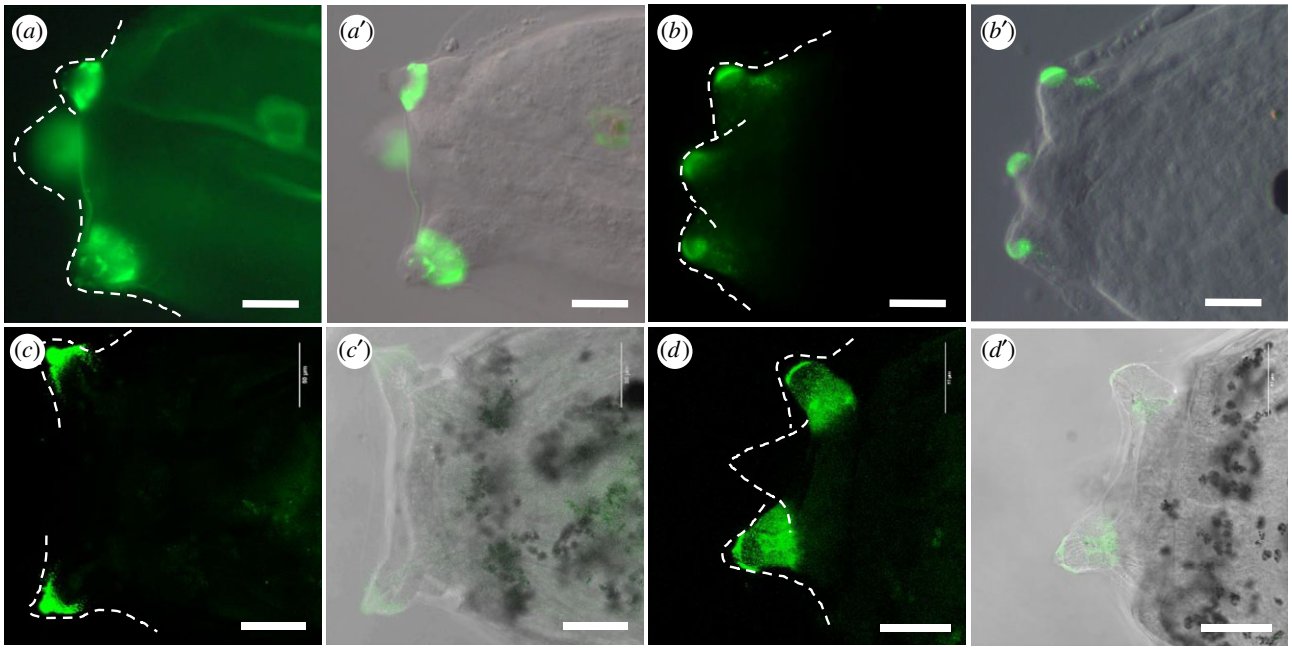

Figure 3. Conserved occurrence of PNA and PHAL-E bound carbohydrates in the larval adhesive organs of *Phallusia mammillata* and *Botryllus schlosseri*. Confocal images of adhesive papillae of *Phallusia mammillata* (*a–b*′) and *Botryllus schlosseri* (*c–d*′) stained by PNA (*a*,*c*) and PHAL-E (*b*,*d*) with the corresponding overlays in DIC (differential interference contrast; *a*′*–d*′). Dotted lines outline the papillae. Scale bar: (*a–b*′) 20 µm, (*c–d*′) 50 µm. (Online version in colour.)

The nitroblue tetrazolium (NBT) substrate staining revealed a strong presence of DOPA in the test cells that surround the tunic (figure 5*a*, control in figure 5*b*) and are enriched in the anterior region surrounding the adhesive organs (rectangle in figure 5*a* and enlarged in figure 5*g*). To have a better view of the papillae, we removed the test cells by dechorionation after fertilization. In dechorionated larvae with test cells removed, we could not detect any NBT staining not even in the papillae (figure 5*d*). Using the DOPA-specific antibody, we verified the presence of DOPA by immunofluorescence in the test cells (figure 5*e*, *e*′) and an expected signal loss in dechorionated larvae (figure 5*f*, *f*′). We confirmed DOPA presence in test cells at earlier stages using both staining methods, notably on fertilized eggs (electronic supplementary material, figure S4) and earlier stage larvae (electronic supplementary material, figure S5).

Interestingly, in anti-DOPA antibody stainings of wild-type larvae, we detected an additional domain resembling a

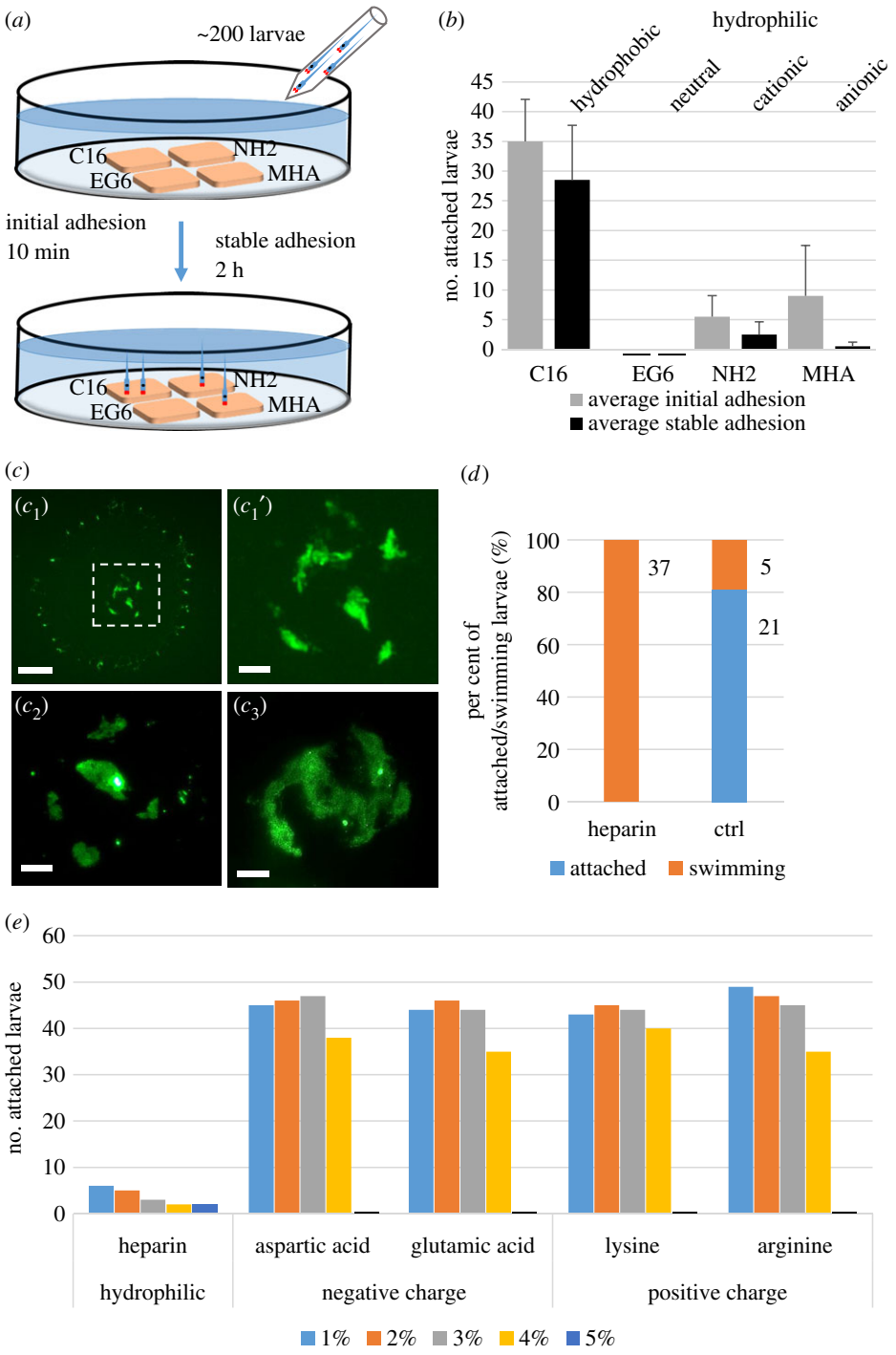

Figure 4. Influence of hydrophilicity but not charge on larval attachment. Adhesion tests of *C. intestinalis* larvae on different SAM surfaces (*a–c*) and in seawater containing heparin or charged amino acids (*d*,*e*). (*a*) Experimental set-up to compare the preference of *Ciona* larvae to settle on different SAMs: 200 larvae added in the seawater could choose between four SAMs placed on an agarose-coated Petri dish. Initial and stable adhesion was counted after 10 min and 2 h, respectively. (*b*) Numbers of larvae attached to a hydrophobic (C16) or three hydrophilic surfaces, i.e. neutral (EG6), cationic (NH2) or anionic (MHA) hydrophilic SAMs. (*c*) PNA-fluorescence images of adhesive plaques on a hydrophobic surface (c_1), with the rectangular central area enlarged (c_1'), or on the hydrophilic cationic (c_2) and anionic surface (c_3). (*d*) Numbers and per cent of attached and swimming larvae in plastic Petri dishes supplied with 2.5% heparin in seawater compared to control seawater. (*e*) Number of attached larvae supplied with increasing concentrations (1–5%) of heparin or of charged amino acids: aspartic acid, glutamic acid, lysine or arginine, respectively. Scale bars: (c_1) 20 µm, (c_1', c_2, c_3) 10 µm. (Online version in colour.)

graded DOPA accumulation at the level of the adhesive papillae (figure 5*h*; electronic supplementary material, movie S2) and in cells that may represent the collocytes by their apically rounded shape [13]. Furthermore, in the adhesive plaques, we detected a weak NBT signal for DOPA (figure 5*i*) that partially overlapped with the fluorescent PNA staining (figure 5*j*,*k*). Anti-DOPA antibody staining confirmed the DOPA presence in the adhesive prints (figure 5*l–n*). Taken together, these data suggest that a DOPA reservoir is provided by the test cells to feed the adhesive papillae that may actively take up DOPA. The presence of DOPA in the adhesive plaque may point to a role in plaque cohesion.

3. Discussion

We provide evidence that specific sugar residues, hydrophobicity, heparin-like molecules and catechols may play a role in regulating tunicate larval adhesion.

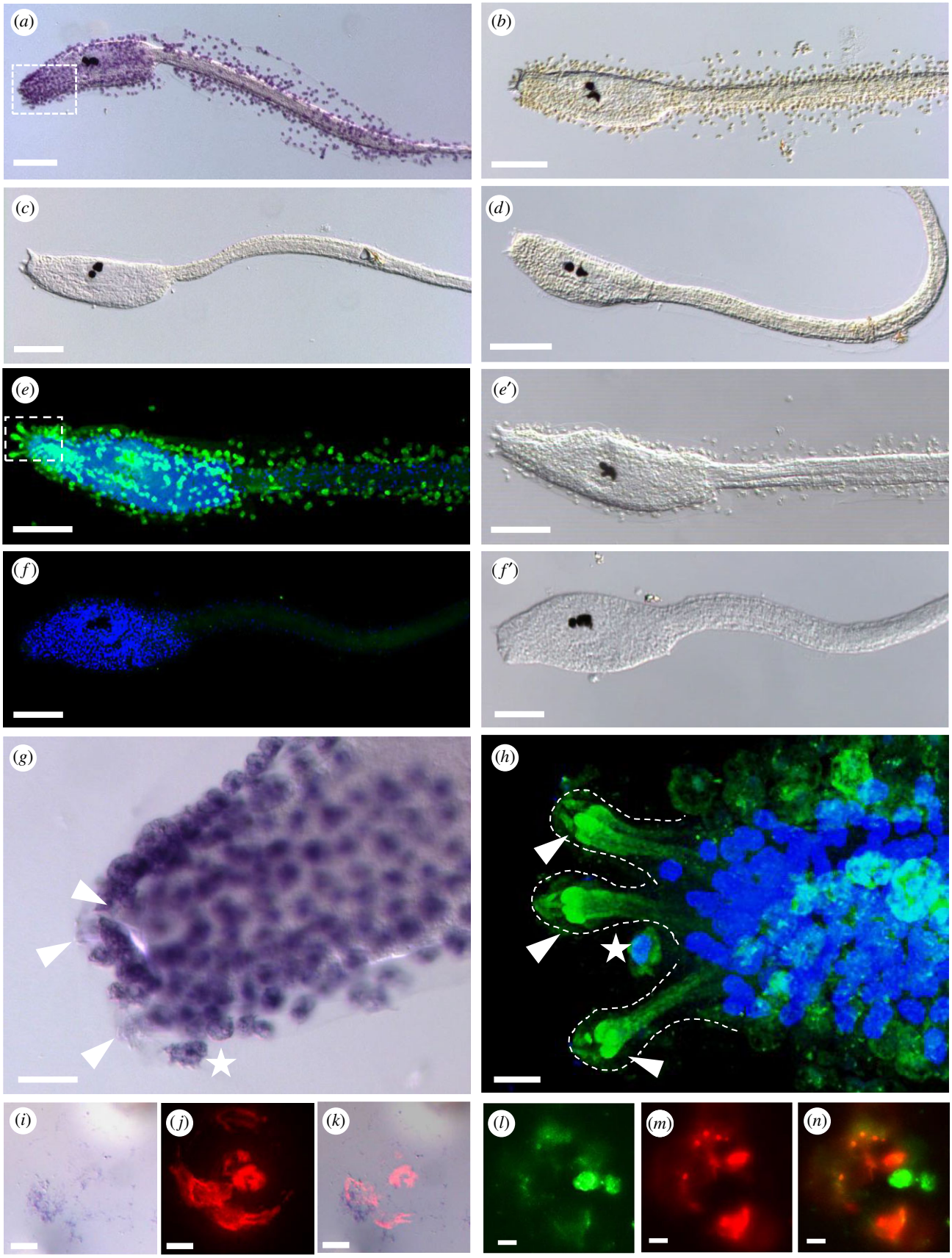

Figure 5. DOPA presence in test cells, papillae and adhesive plaques of chorion containing larvae. (*a–d*,*g*) DOPA-NBT staining and (*e-f*′,*h*) anti-DOPA-antibody fluorescent staining of *Ciona* larvae. (*a*) NBT staining visible in chorionated larvae, is absent upon dechorionation (*c*) and in controls without substrate (*b*,*d*). (*e*) Double fluorescent labelling with (green) anti-DOPA-antibody and (blue) nuclear DAPI labelling of a chorion containing larva showing the tunic surrounding test cells (*e*′). (*f*) Double fluorescent staining of a dechorionated larva having lost both, the DOPA fluorescence and the test cells (*f*′). (*g*,*h*) Details of DOPA stainings around the adhesive organs in NBT (*g*) or antibody labelled larvae (*h*), respectively. The areas of enlargement are marked by rectangles in (a) and (*e*). Arrowheads mark the papillae, white stars the DOPA-containing cells in papillar vicinity. (*i–k*) Adhesive plaque staining with NBT (*i*) and PNA-fluorescence (*j*), and in the overlay (*k*). (*l–n*) Adhesive plaque staining with anti-DOPA-antibody (*l*) and PNA-fluorescence (*m*), and in the overlay (*n*). Dotted lines outline the papillae. Scale bars: (*a–h*) 100 µm, (*g*) 20 µm, (*h–k*) 10 µm. (Online version in colour.)

As glycan decipherers on *Ciona* larvae at the attachment-competent stage we used 21 different lectins and detected the binding of 16 lectins, but only 3 of them (PNA, PHA-E and GSL II) strongly labelled the papillae and the adhesive plaques of *C. intestinalis*. Notably, PNA and PHA-E had little or no cross-reactivity with other tissues, respectively. The majority of the remaining lectins mostly labelled the tunic.

The chemical nature of the lectin specificities (table 1; [19,20]) reveals that the papillary secretions use both O-glycans (PNA) and N-glycans (PHA-E, GSL II) with terminal galactoses and N-acetylglucosamines, respectively, that are not sialylated (no reaction with MAL II). Surprisingly, unlike PNA, jacalin binding is not enriched in papillae as would be expected from a shared specificity for Galß1-3GalNAc. We presently can only speculate whether PNA untypically recognizes Galß1-4GlcNAc (aka. LacNAc, N-acetyllactosamine) to which it binds with a lower affinity [21] but that is not recognized by jacalin [22]. This is consistent with lactose inhibiting PNA binding [23]. ECL and RCA I, however, despite a shared specificity for terminal Galß1-4GlcNAc, did not bind to papillae, which may be explained by their preference for branched biantennary glycosides [24,25]. Clearly, quite sophisticated inhibition studies will be required to resolve this issue in the future. Interestingly, a unique specificity of bisected complex N-glycans in papillae (PHA-E but not PHA-L) is opposed to non-bisecting, branched complex N-glycans in the tunic (ConA) that are densely packed with GlcNAc residues and core-fucosylated (LCA and PSA). The N- and O-glycans of the tunic seem to lack terminal ßGal/ßGalNAc residues (negative for RCAI, SJA, ECL/ECA) and are likely sialylated (jacalin but not PNA). Uniquely, likely O-glycan decorations were found on cellular nuclei (terminal fucosylation on Gal residues, UEA-I) and on the axial structures, notochord and nerve cord (sialylated Gal/GalNAc, EBL/SNA). These very separate sugar decorations are likely a reflection of the different functions of the underlying tissues. Ongoing work will determine which proteins are involved and how the specific carbohydrate moieties could contribute to the adhesive properties.

Strikingly, PNA and PHA-E binding are also localized to adhesive papillae in two phylogenetically distant tunicate species. Further experiments will determine the cellular and subcellular localization in *Phallusia mammillata* and *Bortyllus schlosseri*. We have previously shown that PNA is localized to the adhesive-secreting collocytes. Intriguingly, *Bortyllus* larvae were proposed to have a different composition of cell types, supposedly lacking secretive cells in the papillae [26]. Comparing these species should reveal the specific roles of carbohydrate-containing molecules in the larval attachment.

The glycan patterns found in the ascidian larval adhesive differ from the carbohydrate residues found in secretions of other marine species. Notably, temporary adhesives used for the locomotion of echinoderms, flatworms and *Hydra*, and in defence strategies in cephalopods have been previously screened for specific glycans [27–31]. In all of the latter, however, N-glycosylation and sialylated O-glycosylation seem prevalent in the adhesives (ConA, WGA and jacalin, UEAI, respectively). Consistently, a recent phylogenetic survey of glycan evolution around glycosyltransferases (GTs) postulates that ascidians have evolved with a rather reduced set and many of the decorating final GTs (class 1) that add sialyl or fucosyl groups in the *trans*-Golgi network are missing [32]. While the role of N-glycans in marine bioadhesion is largely unknown, it was proposed that they may mediate the contact of soft tissue with non-living material like in the case of ConA-bound glycans of the mussel tissue interacting with the stiff byssus thread [33]. PNA-bound O-GalNAc glycans, on the other hand, are well-known compounds of epithelial mucins with anti-infectious effects and, due to their hydrophilic nature, are majorly involved in the viscosity and adhesiveness of mucus [34]. PNA-bound glycans are present in ascidian as well as in flatworm adhesives (present study and [13,29] but their exact role awaits clarification.

We showed that the adhesive capacity of *Ciona* larvae is negatively influenced by strongly hydrophilic surfaces, or by the addition of hydrophilic substances to the medium, in our case the highly hydrophilic heparin. Because we did not see any larvae settling on the hydrophilic neutral surface, it is likely that tunicate larvae are unable to displace water from this surface to deposit their glue. Using the SAMs of defined chemical nature we were able to show that *Ciona* larval attachment and deposition of adhesive material is incompatible with strongly wetted neutral surfaces (EG6) while larvae were capable of settling on other substrates. Such antifouling effect of highly hydrated surfaces was described previously for algal spores and bacteria, but also very recently for flatworms [7,15,17,35]. By contrast, on hydrophilic SAMs with charged residues (NH_2 and MHA) with the larvae were able to initially attach and deposit glue but detached again over time. Consistently, charged amino acids did not block the *Ciona* larval adhesion. This contrasts with the situation in flatworms where both heparin and negative charge can influence adhesion [7]. We further show that added heparin changed the surface properties from hydrophobic plastic to render it hydrophilic and thus inhibited *Ciona* larval adhesion.

Our finding of heparin influencing adhesion is consistent with previous studies finding heparin-like substances in test cell granules of ascidian oocytes [36], and suggestions that test cell secretions of acidic (often sulphated) glycosaminoglycans [37] render the outer tunic more hydrophilic to allow for larval swimming in the water [38] up to the point where the outer tunic is cast off at the end of tail resorption. A further interesting aspect of heparin is its storage property for mediators and enzymes that is likely conserved in ascidians [36]. Overall, these observations point to a role of heparin in counteracting fast adhesion of larvae to any type of substrate and allows for prolonged swimming and exploring the substrate prior to permanent attachment.

DOPA is an essential component of mussel adhesives (reviewed in [1]). Consistent with a cohesive/adhesive function in tunicate larvae, DOPA and TOPA (2,4,5-trihydroxyphenylalanine) residues are known components of blood cells populating the adult tunic that contribute to wound healing [18] and are present in the adult adhesive extensions of the tunic [39,40]. In mussels, DOPA residues are a major component of their adhesive proteins and contribute to the byssus thread hardening and are therefore widely used in mussel-mimetic glues (reviewed in [2]). Consequently, DOPA and TOPA residues were recently proposed in tunicate-inspired glues towards restorative tissue medicine [41,42].

To our knowledge, this study is the first demonstration that test cells are an important reservoir for L-DOPA and

that *Ciona* larvae perform a remarkable uptake of L-DOPA through their adhesive organs. We cannot at this point be sure about the uptaking cell type, which is an issue that awaits further analysis.

Interestingly, test cells (thus containing both heparin and L-DOPA) accumulate in the papillary area during the maturation of adhesion_competent larvae [43]. Consistent with a possible role of test cells in adhesion (and subsequent metamorphosis), we found dispersed test cells and their contents (L-DOPA) in the adhesive plaques. Although we can confirm that shedding of the test cells by artificial dechorionation has only minor effects on attachment itself [44], we do note a prolonged swimming behaviour and much delayed tail retraction in subsequent metamorphosis steps as reported. It is unknown how test cell contents could link settlement to subsequent metamorphosis in molecular terms. L-DOPA is also a precursor for neurotransmitters such as dopamine and adrenaline/noradrenaline, and the latter trigger tail absorption during the ascidian metamorphosis [45]. Furthermore, a DOPA-modifying enzyme, *Cin*-PO2, is expressed in the test cells of oocytes and early embryonic stages but the mRNA is actively exported into the neighbouring epidermis cells [46] likely allowing for the accumulation of DOPA in these cells. It is, therefore, very tempting to hypothesize that a separate DOPA reservoir could fulfil a dual role in both the cohesive/adhesive properties for the larval glue as well as in synchronizing attachment with metamorphosis events. Non-neural catecholaminergic storage compartments are found in other marine organisms [1,47,48] and could, more generally, link adhesion to neural functions.

4. Methods

(a) Animal and larvae

Adults of *Ciona intestinalis* and *Pallusia mammillata* were purchased from the Roscoff Marine Station of the Sorbonne University, France, and cultivated in an aquarium with circulating and oxygenated artificial seawater at 16°C until use. Fertilization and embryo culturing were performed as described [49], and embryos were developed on 10 cm Petri dishes coated with 1% agarose in filtered artificial seawater with HEPES (ASWH or ASW) to 18–24 hpf (hours post fertilization).

(b) Lectin fluorescence histochemistry

Botryllus schlosseri larvae (kindly provided by Stefano Tiozzo) were fixed in 4% paraformaldehyde (PFA) for 2 h at room temperature, transferred and kept in 1× phosphate-buffered saline (PBS) until use. Larvae of *C. intestinalis* and *P. mammillata* or their adhesive plaques were fixed in 4% PFA in PBS for 30 min and kept in 1× PBS until use. Lectin labelling was performed as described previously [13]. Biotinylated PNA, PHA-E, GSL II, DSL, WGA, ConA, GSL I, jacalin, LCA, SBA, STL, VVL, LEL, PSA, UEA I, EBL, ECL, RCA I, MAL II, PHAL-L and SJA (Vector Laboratory) were used at a final concentration of 25 µg ml^{-1}.

(c) Immunofluorescence staining of larvae

Tadpole larvae of *C. intestinalis* were fixed as described above then gradually dehydrated to 100% menthol and stored at −20°C. After stepwise rehydration in PBS, specimens were permeabilized with 0.1% (w/v) Triton X-100 in PBS (PBS-T) and blocked in 3% (w/v) bovine serum albumin (BSA) in PBS-T for 2 h at room temperature and incubated in primary antibody rabbit-anti-DOPA (Abcam, ab6426) diluted 1 : 600 in 3% BSA-PBS-T and incubated overnight at 4°C. After several washing steps with PBS-T at room temperature for 2 h, samples were incubated in secondary antibody goat anti-rabbit Alexafluor 488 (Life Technologies, A31627) diluted 1 : 500 in 3% BSA-PBS-T at room temperature for 1 h in dark. Nuclear staining with DAPI (Sigma, D9542) was at 0.035 µg ml^{-1} incubated together with the secondary antibody. Double labelling of PNA lectin and anti-DOPA antibody was performed simultaneously in 3% BSA-PBS-T at the above-described dilutions and using Texas Red Streptavidin (Vector Laboratory, SA-5006) diluted 1 : 500.

(d) Scanning electron microscopy

Ciona intestinalis larvae were allowed to attach completely to round glass and plastic cover slips. After full attachment specimens were fixed with 2.5% glutaraldehyde in 0.1 M cacodylate buffer containing 10% sucrose at 4°C for 1 to 2 h, rinsed with buffer and post fixed in 1% osmium tetroxide in 0.05 M cacodylate for 1 h at 4°C, dehydrated with a methanol series, critical point dried (Pelco, USA) and sputtered with gold. Samples were examined with a Zeiss DSM950 SEM (Zeiss, Germany) and images were taken with a Pentax digital camera and PK_Tether 0.7.0 free software.

(e) Nitroblue tetrazolium staining

One-cell stage embryos and larvae were fixed as described above, washed in 1x PBS for 1 h, incubated with 0.24 mM nitroblue tetrazolium (NBT) and 20 mM Na-benzoate (as a phenoloxidase inhibitor) in potassium glycinate solution, which was prepared by 15% glycine dissolved with 2 M KOH and adjusted to pH 10 [50]. PNA and NBT double-staining of adhesive plaques was performed sequentially, first labelling with PNA as in §4a followed by NBT staining.

(f) Self-assembled monolayers

SAMs were prepared as described previously [7]. Briefly, Si(100) wafers or Schott Nexterion glass substrates were gold-coated in an electron-beam evaporation system preceded by a Ti adhesion layer. The gold-coated substrates were cleaned in a 1 : 1 : 5 solution of 25% NH_3, 30% H_2O_2 and water immediately before immersion in thiol solutions, and then incubated in 50 µM thiol solutions in ethanol (99.5%; Solveco) for at least 24 h in the dark. After incubation, the surfaces were rinsed with ethanol, ultrasonicated in ethanol for 2 min to remove any physisorbed layers, and dried under a stream of nitrogen gas. The resulting SAMs were evaluated by ellipsometry and contact angle measurements. The following thiols were used to form SAMs: $HS(CH_2)_{15}CH_3$ (1-hexadecanethiol, C16; Fluka), $HS(CH_2)_{15}COOH$ (16-mercaptohexadecanoic acid, MHA; Sigma-Aldrich), $HS(CH_2)_{16}NH_2$ (16-amino 1-hexadecanethiol, NH2; Prochimia) and $HS(CH_2)_{15}CONH(CH_2CH_2O)_6H$, (EG6) prepared as in Svedhem *et al*. [51]. SAMs were packed under nitrogen and kept in the dark at room temperature until used.

(g) Adhesion and blocking assays

Adhesion assays and blocking assays were generally performed in 3.5 cm polystyrene plastic Petri dishes.

To perform the SAM surfaces adhesion tests, four different surfaces were immersed into ASWH on a 1% agarose-coated 10 cm Petri dish, then around 200 larvae were added, counted for attached larvae 10 min later as initial adhesion, then after 2 h attached larvae were counted again as stable adhesion.

For the heparin block assay, 2 ml of 5% (w/v) heparin (Car Roth, 7692.2) in ASWH was added to a Petri dish, then 2 ml ASWH containing hatching larvae were pipetted to the 5% heparin medium resulting in final concentration of 2.5% heparin. The number of attached larvae was counted after 2 h.

For positively and negatively charged amino acid block assay, 10% (w/v) of heparin (Car Roth, 7692.2), aspartic acid (Sigma-Aldrich, A9256), glutamic acid (Sigma-Aldrich, 49621), lysine (Sigma-Aldrich,L5626) and arginine (Sigma-Aldrich, A5131) were diluted 1 : 10, 1 : 5, 1 : 3.3, 1:2.5 and 1 : 2 respectively in ASWH each containing 60 larvae, and counted 2 h later for attached larvae.

Generally, experiments were performed at least twice with similar results, and counts determined from representative experiments.

Data accessibility. This article has no additional data.

Authors' contributions. F.Z. carried out the molecular laboratory work, participated in data analysis, carried out the statistical analyses, participated in the design of the study and helped draft the manuscript; J.W. carried out molecular laboratory work, participated in data analysis and critically revised the manuscript; W.S. collected SEM data and critically revised the manuscript; T.E. provided SAM material, participated in data analysis and critically revised the manuscript; U.R. conceived the study, designed the study, coordinated the study, participated in data analysis and drafted the manuscript. All authors gave final approval for publication and agree to be held accountable for the work performed therein.

Competing interests. We declare we have no competing interests.

Funding. Research was supported by the Austrian Academy of Sciences ÖAW DOC 24699 (F.Z.), the University Innsbruck Vicerectorate for Research Sonderförderung 214947 (U.R.), the Nachwuchsförderung Universität Innsbruck (F.Z. and J.W.), the Autonome Provinz Bozen (J.W.), and COST actions TD0906 and CA15216 (European Network of Bioadhesion Expertise).

Acknowledgements. We acknowledge Peter Ladurner for helpful discussion and support. We thank Stefano Tiozzo for kindly providing fixed *Botryllus* larvae.

References

1. Waite JH. 2017 Mussel adhesion—essential footwork. *J. Exp. Biol.* **220**, 517–530. (doi:10.1242/jeb.134056)
2. Hofman AH, van Hees IA, Yang J, Kamperman M. 2018 Bioinspired underwater adhesives by using the supramolecular toolbox. *Adv. Mater.* **30**, e1704640. (doi:10.1002/adma.201704640)
3. Kamino K. 2016 Barnacle underwater attachment. In *Biological adhesives*, 2nd edn (ed. AM Smith), pp. 153–176. Cham, Switzerland: Springer Int.
4. Stewart RJ, Wang CS, Song IT, Jones JP. 2017 The role of coacervation and phase transitions in the sandcastle worm adhesive system. *Adv. Colloid Interface Sci.* **239**, 88–96. (doi:10.1016/j.cis.2016.06.008)
5. Flammang P, Demeuldre M, Hennebert E, Santos R. 2016 Adhesive secretions in echinoderms: a review. In *Biological adhesives*, 2nd edn (ed. AM Smith), pp. 193–222. Cham, Switzerland: Springer Int.
6. Lengerer B, Ladurner P. 2018 Properties of temporary adhesion systems of marine and freshwater organisms. *J. Exp. Biol.* **221**, jeb182717. (doi:10.1242/jeb.182717)
7. Wunderer J *et al.* 2019 A mechanism for temporary bioadhesion. *Proc. Natl Acad. Sci. USA* **116**, 4297–4306. (doi:10.1073/pnas.1814230116)
8. Aldred N, Petrone L. 2016 Progress in the study of adhesion by marine invertebrate larvae. In *Biological adhesives*, 2nd edn (ed. AM Smith), pp. 87–106. Cham, Switzerland: Springer Int.
9. Aldred N, Clare AS. 2014 Mini-review: impact and dynamics of surface fouling by solitary and compound ascidians. *Biofouling* **30**, 259–270. (doi:10.1080/08927014.2013.866653)
10. Pennati R, Rothbacher U. 2015 Bioadhesion in ascidians: a developmental and functional genomics perspective. *Interface Focus* **5**, 20140061. (doi:10.1098/rsfs.2014.0061)
11. Sasakura Y, Mita K, Ogura Y, Horie T. 2012 Ascidians as excellent chordate models for studying the development of the nervous system during embryogenesis and metamorphosis. *Dev. Growth Differ.* **54**, 420–437. (doi:10.1111/j.1440-169X.2012.01343.x)
12. Karaiskou A, Swalla BJ, Sasakura Y, Chambon JP. 2015 Metamorphosis in solitary ascidians. *Genesis* **53**, 34–47. (doi:10.1002/dvg.22824)
13. Zeng F, Wunderer J, Salvenmoser W, Hess MW, Ladurner P, Rothbacher U. 2018 Papillae revisited and the nature of the adhesive secreting collocytes. *Dev. Biol.* **448**, 183–198. (doi:10.1016/j.ydbio.2018.11.012)
14. Ulman A. 1996 Formation and structure of self-assembled monolayers. *Chem. Rev.* **96**, 1533–1554. (doi:10.1021/cr9502357)
15. Callow ME, Callow JA, Ista LK, Coleman SE, Nolasco AC, Lopez GP. 2000 Use of self-assembled monolayers of different wettabilities to study surface selection and primary adhesion processes of green algal (Enteromorpha) zoospores. *Appl. Environ. Microbiol.* **66**, 3249–3254. (doi:10.1128/AEM.66.8.3249-3254.2000)
16. Ederth T *et al.* 2011 Resistance of galactoside-terminated alkanethiol self-assembled monolayers to marine fouling organisms. *ACS Appl. Mater. Interfaces* **3**, 3890–3901. (doi:10.1021/am200726a)
17. Di Fino A, Petrone L, Aldred N, Ederth T, Liedberg B, Clare AS. 2014 Correlation between surface chemistry and settlement behaviour in barnacle cyprids (*Balanus improvisus*). *Biofouling* **30**, 143–152. (doi:10.1080/08927014.2013.852541)
18. Taylor SW. 1997 New perspectives in the chemistry and biochemistry of the tunichromes and related compounds. *Chem. Rev.* **97**, 333–346. (doi:10.1021/cr940467q)
19. Kuno A, Uchiyama N, Koseki-Kuno S, Ebe Y, Takashima S, Yamada M, Hirabayashi J. 2005 Evanescent-field fluorescence-assisted lectin microarray: a new strategy for glycan profiling. *Nat. Methods* **2**, 851–856. (doi:10.1038/nmeth803)
20. Esko JD, Bertozzi C, Schnaar RL. 2015 Chemical tools for inhibiting glycosylation. In *essentials of glycobiology* (eds A Varki *et al.*), pp. 701–712. Cold Spring Harbor, NY: Cold Spring Harbor Laboratory Press.
21. Pereira ME, Kabat EA, Lotan R, Sharon N. 1976 Immunochemical studies on the specificity of the peanut (*Arachis hypogaea*) agglutinin. *Carbohydr. Res.* **51**, 107–118. (doi:10.1016/S0008-6215(00)84040-9)
22. Hagiwara K, Collet-Cassart D, Kobayashi K, Vaerman JP. 1988 Jacalin: isolation, characterization, and influence of various factors on its interaction with human IgA1, as assessed by precipitation and latex agglutination. *Mol. Immunol.* **25**, 69–83. (doi:10.1016/0161-5890(88)90092-2)
23. Cummings RD, Darvill AG, Etzler ME, Hahn MG. 2015 Glycan-recognizing probes as tools. In *Essentials of glycobiology* (eds A Varki *et al.*), pp. 611–625. Cold Spring Harbor, NY: Cold Spring Harbor Laboratory Press.
24. Debray H, Decout D, Strecker G, Spik G, Montreuil J. 1981 Specificity of twelve lectins towards oligosaccharides and glycopeptides related to N-glycosylproteins. *Eur. J. Biochem.* **117**, 41–55. (doi:10.1111/j.1432-1033.1981.tb06300.x)
25. Debray H, Montreuil J, Lis H, Sharon N. 1986 Affinity of four immobilized *Erythrina* lectins toward various N-linked glycopeptides and related oligosaccharides. *Carbohydr. Res.* **151**, 359–370. (doi:10.1016/S0008-6215(00)90355-0)
26. Manni L, Lane NJ, Joly JS, Gasparini F, Tiozzo S, Caicci F, Zaniolo G, Burighel P. 2004 Neurogenic and non-neurogenic placodes in ascidians. *J. Exp. Zool. B Mol. Dev. Evol.* **302**, 483–504. (doi:10.1002/jez.b.21013)
27. Hennebert E, Wattiez R, Flammang P. 2011 Characterisation of the carbohydrate fraction of the temporary adhesive secreted by the tube feet of the sea star *Asterias rubens*. *Mar. Biotechnol.* **13**, 484–495. (doi:10.1007/s10126-010-9319-6)
28. Lengerer B, Bonneel M, Lefevre M, Hennebert E, Leclere P, Gosselin E, Ladurner P, Flammang P. 2018 The structural and chemical basis of temporary adhesion in the sea star *Asterina gibbosa*. *Beilstein J. Nanotechnol.* **9**, 2071–2086. (doi:10.3762/bjnano.9.196)
29. Lengerer B, Hennebert E, Flammang P, Salvenmoser W, Ladurner P. 2016 Adhesive organ regeneration in

Macrostomum lignano. *BMC Dev. Biol.* **16**, 20. (doi:10.1186/s12861-016-0121-1)

30. von Byern J, Rudoll L, Cyran N, Klepal W. 2008 Histochemical characterization of the adhesive organ of three *Idiosepius* spp. species. *Biotechnic. Histochem.* **83**, 29–46. (doi:10.1080/10520290801999316)
31. von Byern J, Cyran N, Klepal W, Nodl MT, Klinger L. 2017 Characterization of the adhesive dermal secretion of *Euprymna scolopes* Berry, 1913 (Cephalopoda). *Zoology* **120**, 73–82. (doi:10.1016/j.zool.2016.08.002)
32. Tomono T, Kojima H, Fukuchi S, Tohsato Y, Ito M. 2015 Investigation of glycan evolution based on a comprehensive analysis of glycosyltransferases using phylogenetic profiling. *Biophys. Physicobiol.* **12**, 57–68. (doi:10.2142/biophysico.12.0_57)
33. Yoo HY *et al*. 2016 Sugary interfaces mitigate contact damage where stiff meets soft. *Nat. Commun.* **7**, 11923. (doi:10.1038/ncomms11923)
34. Brockhausen I, Stanley P. 2015 O-GalNAc glycans. In *Essentials of glycobiology* (eds A Varki *et al.*), pp. 113–123. Cold Spring Harbor, NY: Cold Spring Harbor Laboratory Press.
35. Schilp S, Kueller A, Rosenhahn A, Grunze M, Pettitt ME, Callow ME, Callow JA. 2007 Settlement and adhesion of algal cells to hexa(ethylene glycol)-containing self-assembled monolayers with systematically changed wetting properties. *Biointerphases* **2**, 143–150. (doi:10.1116/1.2806729)
36. Karamanou K, Espinosa DCR, Fortuna-Costa A, Pavao MSG. 2017 Biological function of unique sulfated glycosaminoglycans in primitive chordates. *Glycoconj. J.* **34**, 277–283. (doi:10.1007/s10719-016-9728-5)
37. Materazzi G, Vitaioli L. 1969 Further cytochemical studies of the mucopolysaccharides of the test cells of *Ciona intestinalis* L. *Histochemie* **19**, 58–63. (doi:10.1007/BF00305962)
38. Cloney RA, Hansson LJ. 1996 Ascidian larvae: the role of test cells in preventing hydrophobicity. *Acta Zool.* **77**, 73–78. (doi:10.1111/j.1463-6395.1996.tb01253.x)
39. Ueki T, Koike K, Fukuba I, Yamaguchi N. 2018 Structural and mass spectrometric imaging analyses of adhered tunic and adhesive projections of solitary ascidians. *Zoolog. Sci.* **35**, 535–547. (doi:10.2108/zs180051)
40. Li S, Huang X, Chen Y, Li X, Zhan A. 2019 Identification and characterization of proteins involved in stolon adhesion in the highly invasive fouling ascidian *Ciona robusta*. *Biochem. Biophys. Res. Commun.* **510**, 91–96. (doi:10.1016/j.bbrc.2019.01.053)
41. Oh DX, Kim S, Lee D, Hwang DS. 2015 Tunicate-mimetic nanofibrous hydrogel adhesive with improved wet adhesion. *Acta Biomater.* **20**, 104–112. (doi:10.1016/j.actbio.2015.03.031)
42. Sanandiya ND, Lee S, Rho S, Lee H, Kim IS, Hwang DS. 2019 Tunichrome-inspired pyrogallol functionalized chitosan for tissue adhesion and hemostasis. *Carbohydr. Polym.* **208**, 77–85. (doi:10.1016/j.carbpol.2018.12.017)
43. Sato Y, Terakado K, Morisawa M. 1997 Test cell migration and tunic formation during post hatching development of the larva of the ascidian, *Ciona intestinalis*. *Dev. Growth Differ.* **39**. 117–126. (doi:10.1046/j.1440-169x.1997.00013.x)
44. Sato Y, Morisawa M. 1999 Loss of test cells leads to the formation of new tunic surface cells and abnormal metamorphosis in larvae of *Ciona intestinalis* (Chordata, Ascidiacea). *Dev. Genes Evol.* **209**, 592–600. (doi:10.1007/s004270050293)
45. Kimura Y, Yoshida M, Morisawa M. 2003 Interaction between noradrenaline or adrenaline and the β1-adrenergic receptor in the nervous system triggers early metamorphosis of larvae in the ascidian, *Ciona savignyi*. *Dev. Biol.* **258**, 129–140. (doi:10.1016/S0012-1606(03)00118-0)
46. Parrinello D, Sanfratello MA, Vizzini A, Cammarata M. 2015 The expression of an immune-related phenoloxidase gene is modulated in *Ciona intestinalis* ovary, test cells, embryos and larva. *J. Exp. Zool. B Mol. Dev. Evol.* **324**, 141–151. (doi:10.1002/jez.b.22613)
47. Jager M, Chiori R, Alie A, Dayraud C, Queinnec E, Manuel M. 2011 New insights on ctenophore neural anatomy: immunofluorescence study in *Pleurobrachia pileus* (Muller, 1776). *J. Exp. Zool. B* **316B**, 171–187. (doi:10.1002/jez.b.21386)
48. Pires A, Hadfield MG. 1991 Oxidative breakdown products of catecholamines and hydrogen peroxide induce partial metamorphosis in the nudibranch *Phestilla sibogae* Bergh (Gastropoda: Opisthobranchia). *Biol. Bull.* **180**, 310–317. (doi:10.2307/1542402)
49. Kari W, Zeng F, Zitzelsberger L, Will J, Rothbächer U. 2016 Embryo microinjection and electroporation in the chordate *Ciona intestinalis*. *J. Vis. Exp.* **116**, e54313. (doi:10.3791/54313)
50. Ballarin L, Cima F. 2005 Cytochemical properties of *Botryllus schlosseri* haemocytes: indications for morpho-functional characterisation. *Eur. J. Histochem.* **49**, 255–264.
51. Svedhem S, Hollander C-AK, Jing Shi PK, Liedberg B, Svensson SCT. 2001 Synthesis of a series of oligo (ethylene glycol)-terminated alkanethiol amides designed to address structure and stability of biosensing interfaces. *J. Org Chem.* **66**, 4494–4503. (doi:10.1021/jo0012290)